Use of Response Velocity to Calculate Building Strains from Blasting Vibrations

C. H. Dowding
Dept. of Civil & Environmental Engineering, Northwestern University, Evanston, IL, USA
E. W. Diels
Thornton Tomasetti, Milwaukee, WI, USA

ABSTRACT: This paper describes a series of measurements made on a model structure to test the validity of and difficulties involved in calculation of structural strains from measurement of velocity responses from blasting vibrations. These validation studies were prompted by new ability of commercial seismographs to wirelessly time coordinate measurements and recent observation of non-homogeneous response of urban structures to high frequency excitation. The three story model allows validation with responses at higher frequency modes other than that of its fundamental or natural frequency. Concerns addressed in this study include: response of a multi degree of freedom structure to excitation with 1) sinusoidal excitation motions at frequencies at its higher modes of response and 2) blast vibration excitation with dominant frequencies much higher than the system's fundamental or natural frequency; and ability of differential displacements from integrated velocity time histories to replicate the time history and amplitude of strain time histories directly measured with stain gages.

1. INTRODUCTION

This paper describes a series of measurements made on a model structure to verify the validity of and difficulties involved in calculation of structural strains from measurement of velocity responses of buildings to blasting vibrations. These validation studies were prompted by two recent developments in blast vibration monitoring. Commercial seismographs are coming to market with an ability to wirelessly time coordinate measurements which simplifies measurement of differential displacement with velocity transducers. Second, wired, time coordinated measurements of large urban structures to close in blasting (Dowding et al, 2016 and 2018) show non homogeneous responses that are unlike responses of residential structures, which are the basis of most blast vibration monitoring and control. See Appendix B in full article for details of the difference between response of large urban and residential structures to ultra-high frequency excitation motions.

The model structure is a three story or three degree of freedom structure to allow validation with a complex structure that can respond in higher frequency modes other than that of its fundamental or natural frequency. Concerns addressed in this study include: response of a multi degree of freedom structure to excitation with sinusoidal excitation motions at frequencies equal to frequencies of its higher modes of response as well as to a blast vibration with dominant frequencies much higher than the system's fundamental or natural frequency;

Most importantly an assessment is made of the ability of differential displacements from integrated velocity time histories to allow replication of the time history and amplitude of strains by comparison with directly measured strain time histories. This replication is crucial to the use of velocity response measurement as a blast vibration control tool. If strain can be calculated from differential displacement responses calculated from velocity time histories then building velocity response time histories can be employed as a control criteria. Use of differential displacements to calculate inter story shear forces is employed in earthquake engineering, and thus use of differential displacements to calculate strains follows from normal practice in structural dynamics.

The article begins with a detailed description of the procedure to calculate displacement and strain from velocity time histories. Model and system components are then introduced. Method for

calibrating velocity transducers is defined. Strain gages to directly measure bending strains are described. Time histories of model excitation and response are presented. Amplitudes of response are compared and discussed. Strains calculated from both an independent system and a commercial seismograph are compared. Because of space constraints, reference is made to the full report/article (that with Appendices) is available at http://www.iti.northwestern.edu/acm/publications.html.

2. DETERMINATION OF STRAIN FROM INTER STORY DRIFT or DIFFERNTIAL DISPLACEMENT

Strains in walls can be calculated from time correlated structural velocity response time histories through a multi-step process. First the velocity responses are integrated to determine displacements. Determination of the displacement time histories requires correction of baseline irregularities. An example of the four steps in this correction process is shown in Figure 1 (Dowding et al 2016). First, the velocity time history (a in the figure) is baseline corrected. Linear and second order polynomial baseline corrections were tested as shown in (b). As can be seen the polynomial correction did not return the displacement curve to zero at the end of motion. The displacement time history was returned to zero at the end of motion by subtracting the 200 point central-moving– average (continuous line in) (c) to produce the displacement time history that oscillates about zero as shown in (d).

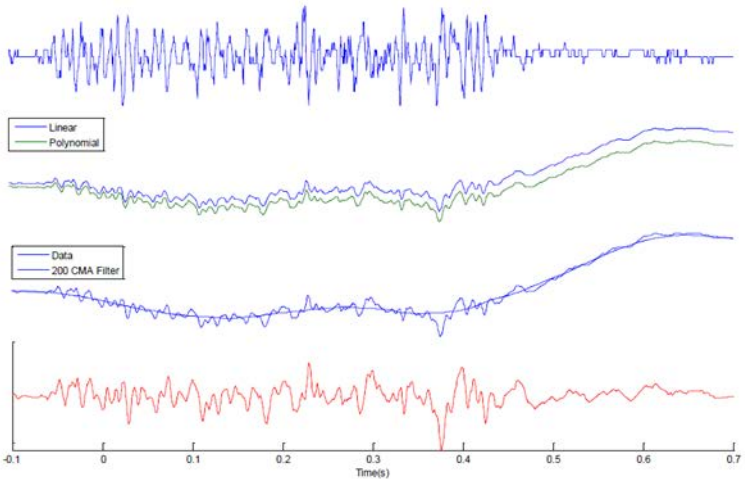

Figure 1. Displacement calculation using baseline correction and 200 point central-moving-average filtering: (a) (top) Velocity recording, (b) Displacement after linear and second order polynomial baseline correction, (c) 200 point central-moving-average filtering of the second order baseline correction displacement, (d) (bottom) final displacement that ends with zero displacement.

While a 200 center point moving average was employed in the example, fewer points (50 to 100) will also allow displacement to come to zero after the excitation. The important criteria is that the time interval over which that average is made should include one to three periods of a mixed frequency pulse's dominant frequency.

Strains are then calculated from differential structure displacements that are obtained through simple subtraction of time correlated structural displacement time histories. These differential displacements are then searched for the largest difference. This maximum differential displacement is transformed into strain as shown below.

Differential displacement, δ_{max}, can be translated into shearing or tensile strains depending on its form. The simplest form of differential displacement is that of translation, shown in the elevation views in Figure 2 (Dowding, 1996). The shearing strain, γ_{max} in the plane of the wall is the angle change and for small angles is

$$\gamma_{max} = \delta_{max}/h,$$

where h is the vertical distance between the two locations at which the response velocities were measured.

Translational bending strains, perpendicular to the wall are also illustrated in Figure 2 and can be estimated from beam theory as

$$\varepsilon_{max} = \sigma_{max}/E = (M_{max}\ d)/EI$$

where M is the maximum moment, d is the distance from the neutral axis to the outer beam fiber (1/2 the wall's thickness), E is Young's modulus of elasticity, and I is the moment of inertia of the beam (a slice of the wall). In this case the beam comprises the entire wall, bricks, wall framing, and interior wall board. Furthermore, the maximum moment can be shown to be

$$M_{max} = (\delta_{max}6EI)/h^2 \text{ or } (\delta_{max}3EI)/h^2$$

for the fixed-fixed or fixed-free restraint conditions, where h is the distance between measurement points. Therefore, the wall bending strains can be estimated by substituting the moment into the strain equation for fixed-fixed and fixed-free respectively

$$\varepsilon_{max} = (\delta_{max}6d)/h^2 \text{ or } (\delta_{max}3d)/h^2$$

Shearing strains are larger than the bending strains as shown by a typical example. A 10 Hz or single story residential structure would sustain a differential displacement of 0.254 mm if excited by a 7 delay quarry blast with a peak particle velocity of 25 mm/s. Thus the shear strain would be

$$\gamma_{max} = \delta_{max}/h = 0.0254 \text{ cm}/300\text{cm} = 100 \times 10^{-6} \text{ cm/cm or } 100\ \mu$$

and the bending strain would be

$$\varepsilon_{max} = (\delta_{max}\ 3 \text{ to } 6\ d)/h^2 = (0.025 \text{ cm}*3 \text{ to } 6*\ 10\text{cm})/300\text{cm}^2 = 13 \text{ to } 26\ \mu$$

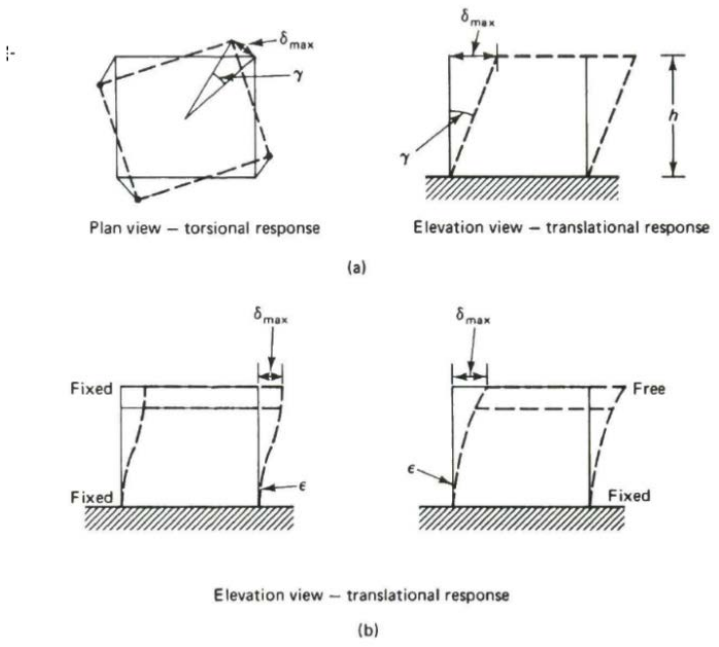

Figure 2 Strain and deflected shape; (a) shearing; (b) bending (Dowding 1996)

3. MODEL FOR VALIDATION OF CALCULATION OF INTER STORY DRIFT

As shown in Figure 3, the model consists of four main components: a model structure, a device to excite the model, and velocity transducers to capture the model's motion, and strain gages to directly measure strain.

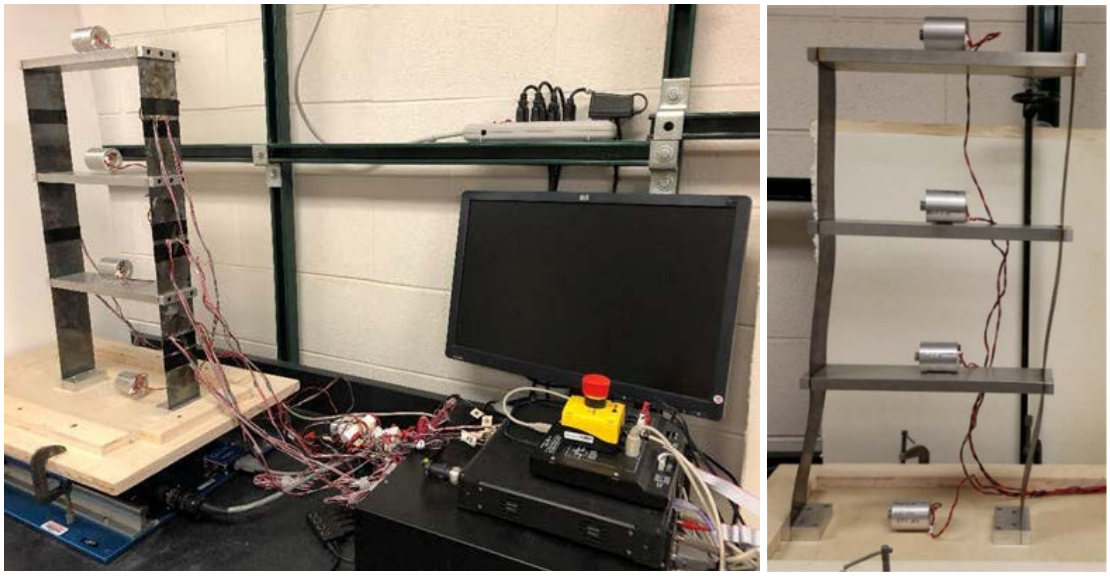

Figure 3: Left testing apparatus consisting of the model structure, input device (here the Shake Table II), and recording devices (velocity transducers recorded by voltage sensors), and strain gages. Right: the deflected shape of the model during excitation at it fundamental mode, 1.88 Hz.

This model allows direct measurement of the bending strain with strain gages and thus validation of calculation of strain through measurement of differential displacement. Accordingly, the discussion will concentrate on bending strains even though they are the smallest of the two types of translational strain. The model structure features all-metal construction with thin, flexible walls and thicker, relatively more massive floors. Approximately 21 cm separate each floor, and floors are 30 cm wide. With three floors above ground level, this model acts as a three degree-of-freedom system with three masses of the same weight at each floor.

Using the optical method described below in the velocity transducer calibration process section, the first three excitation mode frequencies of the structural model were found to be 1.88, 5.43, and 8.24 Hz (Diels, 2018). Damping was measured during free response and was found to be slightly less than 2%. As seen in the photographs, the model has little to no shear resistance, and thus this unusually low damping seems reasonable. Most structures are damped approximately 5%. While the model continued to vibrate long after excitation, real structures do not because of their higher damping (Dowding, 1996).

Excitation was provided by the Quanser Shake Table II, shown at the base of the model in Figure 3 left. According to Quanser, this shake table is rated to drive a 7.5 kg load at 2.5 g and has a maximum displacement of ± 7.62 cm (Quanser, 2017), far above requirements necessary for this research. Power and feedback controllers—along with manufacturer provided control software—direct the shake table's movements. This software provides amplitude and frequency control of excitation for either a sinusoidal time-displacement function or a programmable blast vibration. For this configuration, the model was screwed to a wooden platform, which was clamped securely to the shake table.

Input excitation and structural response was captured with Geospace Technologies HS-1 geophones (velocity transducers). These sensors produce an analog voltage proportional to their excitation velocity. Pasco voltage Analog to Digital (A/D) transform the transducer's analog voltage signal and relayed it digitally to Pasco's Capstone software to record digital voltage time histories. Voltage data were then converted to units of velocity after special calibration described below.

4. VELOCITY TRANSDUCER CALIBRATION PROCESS

Conversion from velocity transducer output voltage to units of velocity is dependent on the excitation frequency experienced by the transducer. The manufacturer provided conversion chart (upper left portion of Figure 4) displays nonlinear response below 10 Hz as shown. Because the first three excitation modes of the structure (1.88, 5.43, and 8.24 Hz) occur below the flat response region, it was necessary to manually calibrate voltage-to-velocity conversion rates. These calibrated conversion rates are shown as the encircled data dots in Figure 4 for the first three excitation modes as well as 12 and 15 Hz.

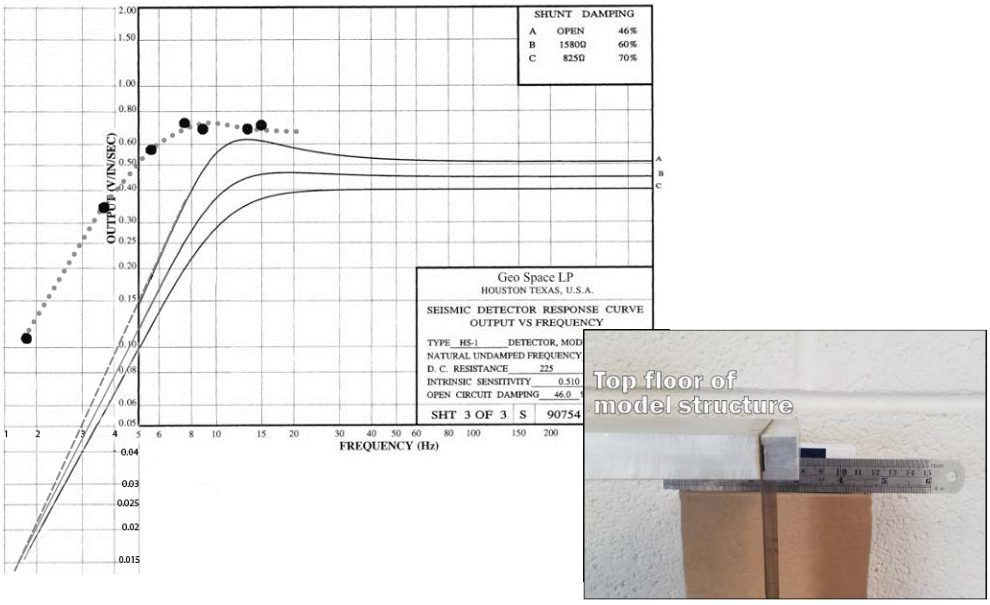

Figure 4: Upper left: velocity transducer conversion chart is taken directly from the velocity transducer manufacturer (HS-1). The encircled points represent conversion rates calculated at various excitation frequencies. INSET- lower right: A ruler positioned behind the top floor was employed to visually measure maximum displacement during excitation and calculate the velocity transducer conversion rate.

Velocity transducers were calibrated independently by visually measuring displacement as shown in the inset in Figure 5 through a trial and recalculation process. First the structure's modal frequencies were found by searching for maximum voltage during structural responses. No conversion factor was necessary since velocity varies directly with output voltage. When the top floor transducer's output voltage amplitude reached a steady maximum, a video of the top floor moving relative to the ruler was recorded to visually measure displacement at the top floor.

Using Figure 4, an initial voltage-to-velocity conversion rate was selected to calculate velocity; time histories of which were subsequently integrated to calculate displacements. Amplitude of this displacement at steady-state was then compared to maximum displacement found from video analysis. The voltage-to-velocity conversion rate was adjusted until displacements integrated from velocities matched those from video analysis.

5. ANALOG TO DIGITAL CONVERSION

PASCO voltage sensors were used to capture and digitize velocity transducer output. These sensors were operated at a sample rate of 500 Hz, much greater than the highest excitation frequency of 30 Hz. Thus at least 16 samples are obtained during the period of a 30 Hz blast vibration pulse. The error in peak capture is less than 5% for this study.

6. STRAIN GAGE INSTALLATION

Rosette strain gages from Micro Measurements were employed to measure column strain from inter story drift or inter story differential displacement. These gages are securely adhered to the metal with resin after a thorough cleaning of the base metal. These rosette gages are made up of three linear gages arranged at 45 degrees to each other. Each rosette was placed approximately 1.75 inches from the nearest point of column fixity; therefore, strains in these gages are directly related to inter story displacement by the same constant. See Appendix A for details. One of the gages was placed at 2 inches from the point of fixity at the base and therefore has a different constant relating strain and inter story drift; this difference is accounted for in data analysis.

Principal strains may be calculated using strains from the three gages in each rosette. Care was taken to place the rosettes aligned with the column, placing one linear gage in parallel with the column. Strain from this linear gage was then compared to calculated principle strain. Error between the two was less than 0.5 %; therefore, it was deemed acceptable to monitor this one channel in each rosette, increasing the system's monitoring capacity to eight gages.

7. MODEL PERTURBATION

The model was perturbed sinusoidally at its three modal frequencies of 1.88, 5.43 and 8.24 Hz. It was also excited with a ~ 15 to 30 Hz dominant frequency motion that simulates a blast vibration time history. These excitation motions are shown in Figure 5. The shake table driving mechanism appears to be a stepping motor as shown by the constant time interval steps.

As can be seen in Figure 5, the shake table’s movement (in terms of velocity excitation) is not purely sinusoidal and takes a non-negligible amount of time and a number of pulses to reach steady-state. Input velocity is obviously not a clean sinusoidal function because of the stepping motor actuation; however, a 60-point moving central average (equating to 0.24 seconds or at a recording rate of 500 samples per second on the 1.88 Hz time history) illustrates the velocity is nearly sinusoidal on average. Other moving point averages are also shown by the thick lines in the figure.

Integration of the excitation velocity to displacement shows that the displacements are sinusoidal at the programmed frequencies (Diels, 2018). This consistent displacement response is also shown in the displacement time histories in Appendix C of the full report. Even though the shake table is unable to immediately produce a constant amplitude, maximum excitation velocities (PPV) reached 4, 11, and 15 mm/s for the three sinusoidal perturbations and 32 mm/s for the blasting vibration within the first one second of excitation. One second of excitation was chosen as the comparative measure since the blasting vibration excitation motion was some 0.75 seconds long.

These sinusoidal model motions were also produced in another earlier experiment with a rotating cam device that was operable at varying frequencies (Diels, 2018). Rotating cam measurements of model velocity response verify observations of excitation and model response reported in this article at the three modal frequencies, 1.88, 5.43 and 8.24 Hz.

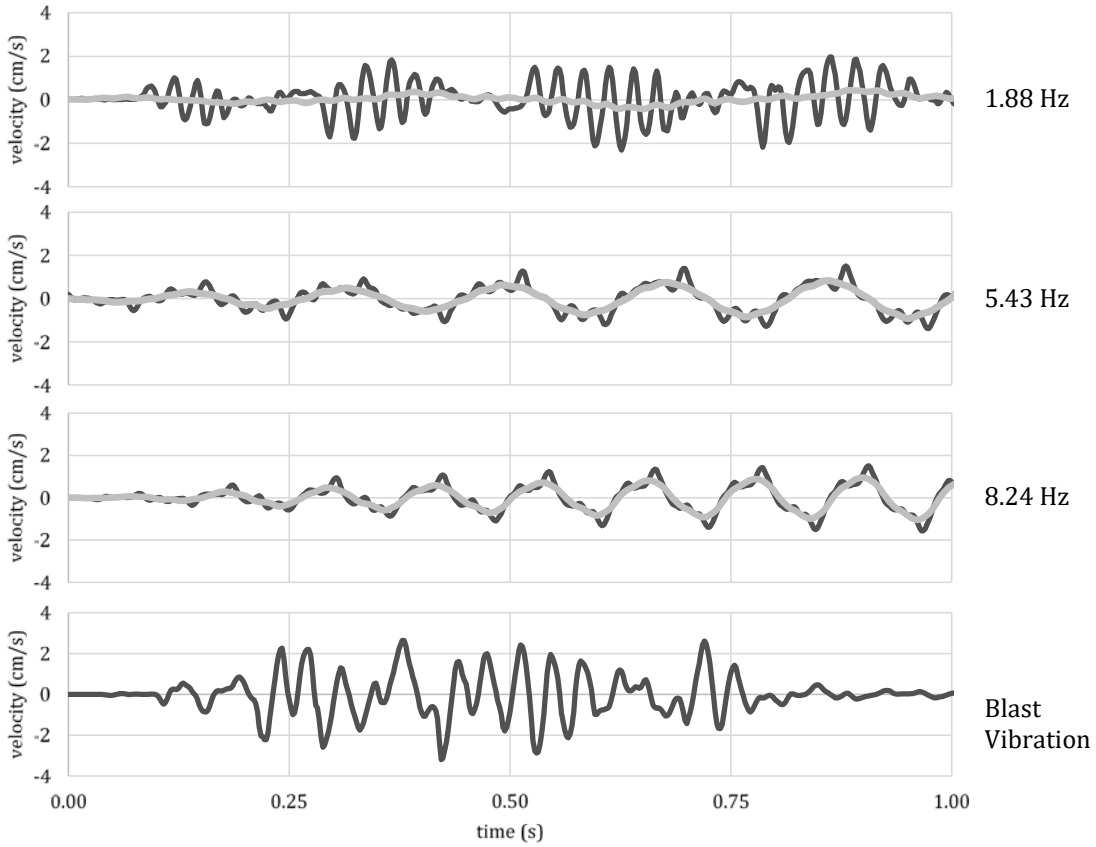

Figure 5. The first 1 second of all four excitation motions: Upper three 1.88 Hz, 5.43 and 8.24 sinusoidal motions: Bottom, blast vibration. The shake table was programmed to produce motions with a maximum displacement of 0.03 cm to fit the limitations of the shake table and velocity transducers. The thick lines display more accurately the average velocities. The smooth displacement time histories are shown in Appendix C of the full report.

8 OUT OF THE PLANE OF THE WALL BENDING STRAINS

Model bending strain response between the first floor, L1, and the ground excitation, G, during the first one second of perturbation is shown in Figure 6. Bending strains were the principal focus of this study because they can be measured directly with strain gages. Since there are no shear walls in this model, shear strain cannot be directly measured.

Despite the increasing peak particle velocity (PPV) of excitation, model response declined with PPV because the exaction occurred at frequencies much higher than the model's fundamental or natural frequency of 1.88 Hz. The maximum directly measured bending strain responses between L1 and G as measured by the strain gages were 20, 22, 15 for the three sinusoidal excitation frequencies, and 11.6 x 10^{-6} mm/mm for the blast vibration with excitation PPV's of 4, 11, 15 and 32 mm/s respectively. The strain in the ground floor wall was the (or nearly the) largest no matter the form of excitation as can be seen in Table 1.

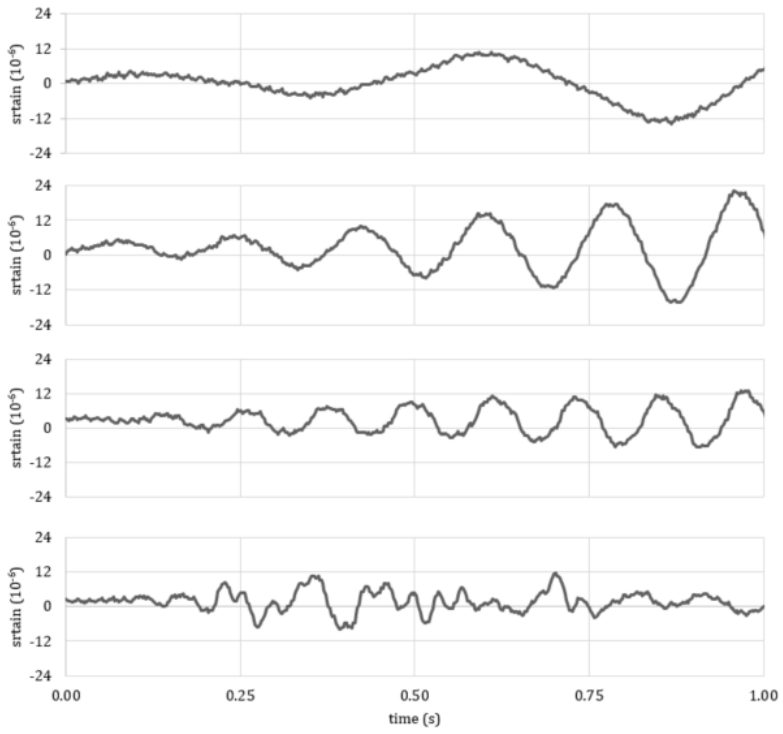

Figure 6: Directly measured bending strains between the 1st floor and the ground were 20, 22, 15, and 11.6 x 10-6 mm/mm from top to bottom for PPV excitation of 4, 11, 15 and 32 mm/s within one second of excitation.

Because use of the stand alone GeoSpace transducers involves a single conversion factor for motion they are best employed in the excitation frequency range where their response is linear. Thus for each of the sinusoidal excitations (1.88, 5.43 & 8.24 Hz) the different, specific conversion factors of 0.04, 0.08, and 0.65 V/in./sec. were employed. A conversion factor of 0.65 V/in./sec. was employed for use with the blast vibration excitation as it appeared that this factor would be constant and appropriate for frequencies between 10 and 30 Hz.

Figure 7 compares time histories of excitation, response displacements and strains at the different levels in the structure for excitation by the 15 to 30 Hz dominant frequency blasting vibration. Of particular importance is the comparison of bending strains calculated through inter story drift and direct measurement. The procedure for calculation strain from inter story differential displacement or drift has been described above. As can be seen in the figure the form of the strain time histories from inter story drift and direct stain measurement is eerily similar.

There are many reasons for the differences in the maximum strains. They include the 4 step baseline correction procedure, type of transducer, transducer response characteristics, single conversion factor with the geospace transducer system, exact location of the strain gage, etc. Sensitivity of the calculated bending strains to changes in the conversion factors, number of points employed in the moving average, and precise location of the strain gages will be discussed in the sensitivity section.

Table 1: Comparison of bending strain responses calculated from inter story drift with that measured by strain gages. Comparison of time histories in figures 7 & 8 shows high correlation of time history form. The amplitudes are the maximum values during the first second of excitation because the blast vibration time history lasts less than one second. Thus energy fed into the system was limited to that during the first one second of perturbation no matter the frequency of excitation.

Velocity Transducers

		Bending Strain Strain (10^{-6})			
		velocity transducers	strain gages	% difference	conversion factor (V/in/s)
Mode 1	L1-G	24	20	20%	
1.88 Hz	L2-L1	12	13	-8%	0.08
ppv = 4 mm/s	L3-L2	14	7	100%	
Mode 2	L1-G	24	22	9%	
5.43 Hz	L2-L1	17	16	6%	0.40
ppv = 11 mm/s	L3-L2	25	23	9%	
Mode 3	L1-G	10	13	-23%	
8.24 Hz	L2-L1	13	15	-13%	0.65
ppv = 15 mm/s	L3-L2	11	15	-27%	
Blast Vibration	L1-G	6.6	11.6	-43%	
max ppv	L2-L1	3.8	8.4	-55%	0.65
= 32 mm/s	L3-L2	6.5	9.5	-32%	

Commercial Seismograph

		Bending Strain Strain (10^{-6})		
		commercial	strain gages	% difference
Blast Vibration	L1-G	7.9	10.6	-25%
max ppv	L2-L1	7.6	9.2	-17%
= 32 mm/s	L3-L2	8.2	9.6	-15%

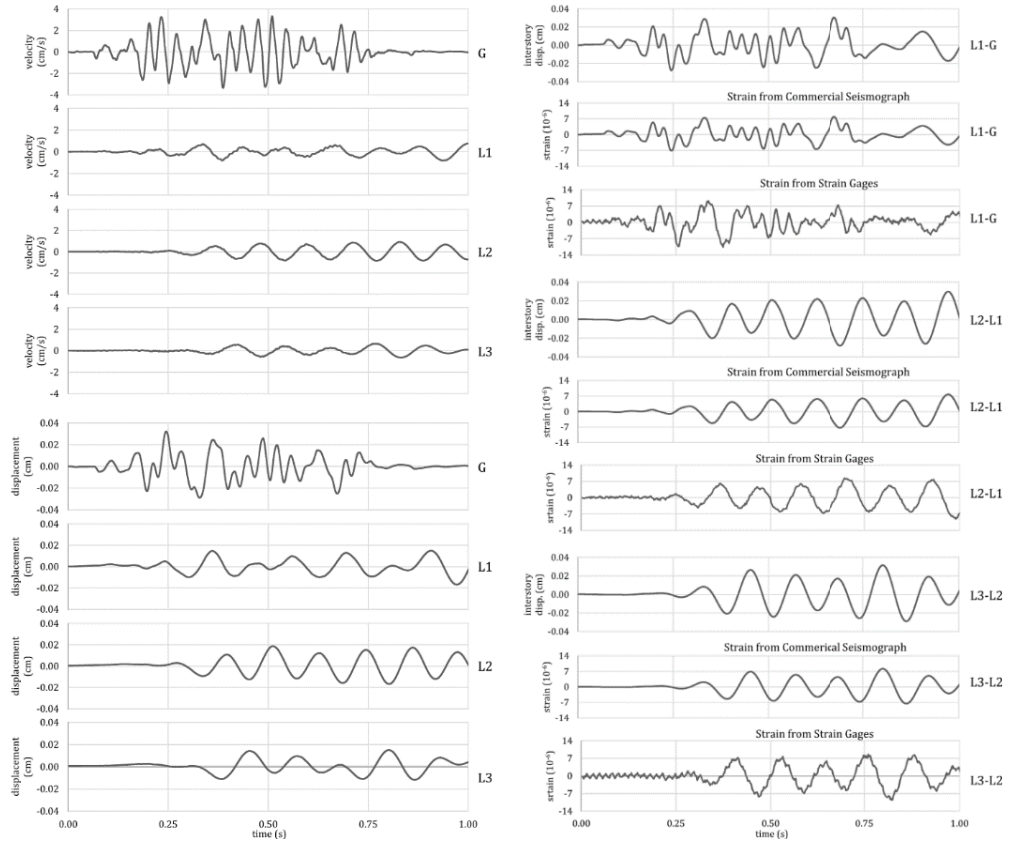

Figure 7 Comparison of time histories of model response featuring the comparison of stains – calculated from inter story differential displacement as measured with the commercial seismograph and that directly measured – at the various inter floor locations: L1-G, L2-L1 and L3-L

9. COMPARISON with MEASUREMENT by COMMERCIAL SEISMOGRAPH

Calculation of strain from inter story drift measured with velocity transducers was also conducted with a commercial seismograph. Commercial seismographs offer an advantage because they automatically compensate for the effects of variable physical transducer response with declining frequency. While the form and magnitude of the compensation will vary by manufacturer, they all offer such compensation.

Figure 8 compares the inter story strains as calculated with the commercial seismograph and those directly measured. Responses for L1-G and L2-L1 are shown because L1-G deformation tends to produce the largest strain, which has also been observed in real structures (Dowding, et al, 2016). L2-L1 strains from the commercial seismograph (commercial) are much closer to those directly measured than were those measured with the Geospace single conversion constant (velocity transducers). As shown in the figure the time history form is quite similar for calculated and directly measured strains. As shown in Table 1, use of commercial seismographs allowed calculation of bending strain peak amplitudes within 15 to 25 % of those directly measured.

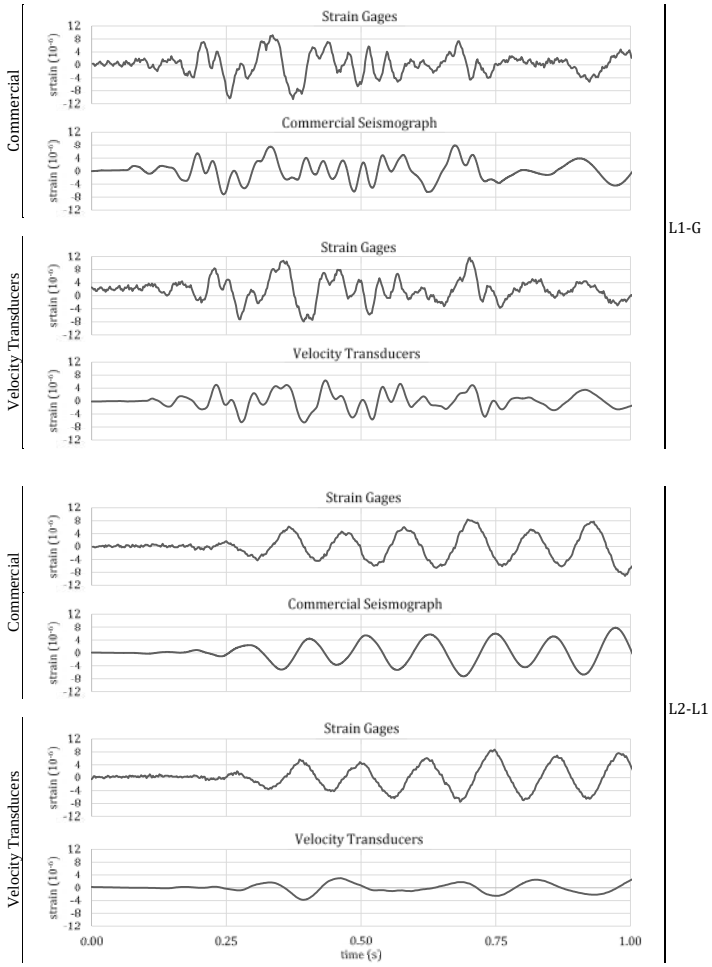

Figure 8 Comparison of strain time histories for wall between floors shows remarkable similarity of detailed form. Commercial seismograph (commercial seismograph) is better able to reproduce strain time histories than the single conversion factor transducers (velocity transducers)

10 IN PLANE SHEAR STRAIN

Since in plane shear strains are larger than out of plane bending strains, it is important to discuss their calculation. Since form and amplitude of structural bending strains has been shown to be calculable from differential displacement there is no reason not to believe that shear strain can also be calculated from differential displacements for models and real structures. Since the calculation relies upon the same maximum differential displacements, δ_{max}, calculation is relatively simple:

$$\gamma_{max} = \delta_{max}/h,$$

where h is the vertical distance between the two locations at which the response velocities were measured.

Even though there is no shear wall on which to measure shear strains, shear stress is still induced between floors, which is resisted by the thin walls of the model which are bent "out of plane" by these shear stresses.

11 SENSITIVITY of CALCULATED BENDING STRAINS

Given the success of calculating bending strain from velocity response, it is important to know the sensitivity to these calculations from changes in either the procedure or parameters employed. Accordingly an investigation was conducted on effects of changes in several key processes and parameters on the differential displacement based, calculated blast vibration induced bending strains between the first floor and the ground (L1-G). Results are summarized in Table 2. Directly measured blast vibration strains are compared for changes in positions of the strain gages that very by 0.5 mm and 1.0 mm from that employed in the main study. Strains from the velocity transducers are compared for number of data points for baseline correction of 50, 60 and 200. No such correction was applied with the commercial seismograph as the software provided performed this procedure automatically. Finally, strains using single conversion factors for Geospasce transducers from specific calibration and that of the manufacturer are compared with those provided by the commercial seismograph.

Table 2: Sensitivity of L1-G bending strains to changes in procedure and parameters with velocity transducers

		Velocity Transducers	
Factor Influencing Strain Calculation		ε (10^{-6})	% difference from baseline
strain gage placement	*+/- 0.5 mm*		+/- 0.87%
	+/- 1.0 mm		+/- 1.7 %
# moving average points for baseline correction	*50 pts*	7.1	8%
	(baseline) 60 pts	6.6	
	200 pts	6.7	1.5%
velocity transducer conversion factor	*commercial seismograph (baseline)*	7.1	
	manufacturer calibrated (0.51 V/in/sec)	8.4	18%
	experimentally calibrated (0.65 V/in/sec)	6.6	-7%

12 CONCLUSIONS

The model behaves in the expected theoretical fashion, where excitation at the same peak particle velocity but with frequencies higher than the fundamental frequency produce lower response both in terms of inter story drift and strain.

For equivalent excitation times, excitation at frequencies higher than the fundamental does not produce larger directly measured strains than at the fundamental for the same peak particle velocity even when the structure is not a single degree of freedom system. Sinusoidal excitation at the second and third modal frequencies of a three degree of freedom system produced strains only 15% greater even when excited at with peak particle velocities 2 to 3 times larger.

Excitation with blast vibration characteristics (15 to 30 Hz dominant frequency) produced maximum directly measured strains that were only some 60% of those produced by an equivalent one second of excitation at the fundamental frequency (1.88 Hz) despite excitation with peak particle velocities that were some 8 times those at the fundamental frequency.

Greatest change in motions tends to occur between the ground excitation and the first floor response, which is also seen in the response of real structures.

Strains can be calculated with inter story drift or differential displacement from velocity measurements within limits.

The form of the strain time histories calculated from inter story drift is similar and almost the same as that from direct measurement.

Increasing the agreement of calculated and directly measured strains above that reported herein requires more work on transducer selection, transducer placement, and baseline correction processes.

REFERENCES

Diels, E.W (2018) Comparison of Measured Model and Theoretical Structural Response to Sinusoidal Excitation Pulses. Internal Report, Department of Civil and Environmental Engineering, Northwestern University, Evanston, Il. Available at http://www.iti.northwestern.edu/acm/publications.html

Dowding, C.H. (1996) Construction Vibrations, Prentice Hall Inc., Englewood Cliffs, NJ, 1996, 620pp

Dowding, C.H., Hamdi, E., & Aimone-Martin, C. T. (2016) Strains Induced in Urban Structures by Ultra-High Frequency Blasting Rock Motions: A Case Study. Rock Mechanics and Rock Engineering, 1-18. DOI: 10.1007/s00603-016-0921-4

Dowding, C.H., Aimone-Martin, C. T, Meins, B.M. & Hamdi, E., (2018) Large Structure Response to High Frequency Excitation from Rock Blasting, International Journal of Rock Mechanics and Mining Sciences, Vol 111, Nov, Pgs 54-63

Appendix A
Reconciliation of Location of Strain Measurement and Differential Displacement

The strain, ϵ, at any point along a fixed-fixed column may be calculated using only column height, h, distance along the column, x, distance from the neutral axis, c, and interstory displacement, Δ. In this study, unless otherwise noted x = 4.45 cm. A brief derivation below shows how strain is calculated from these few parameters. When the location of strain is known (as with a strain gage), Equation (1) directly relates strain and interstory drift with a single constant.

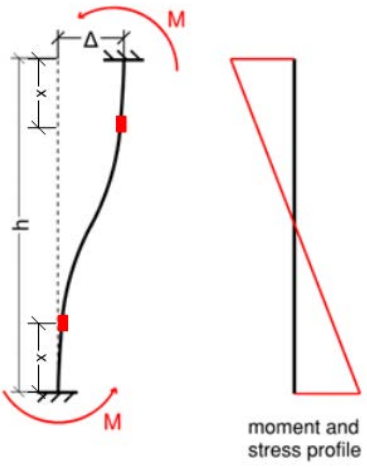

$$M(x) = -M + \frac{2x}{h}M$$

$$M = \frac{6EI}{h^2}\Delta$$

$$\sigma = \frac{Mc}{I}, \qquad \epsilon = \frac{\sigma}{E}$$

$$\epsilon(x) = \frac{6c}{h^2}\left(\frac{2x}{h} - 1\right)\Delta \quad (1)$$

Appendix B
Difference in response of large and small structures to excitation by high and lower frequency pulses by scaled comparison of response of urban structures to high frequency excitation with that of houses to lower frequency mine blast excitation

Figure B1 describes the difference in response of large and small structures to excitation by high and lower frequency pulses by scaled comparison of response of urban structures to high frequency excitation with that of houses to lower frequency mine blast excitation. Scaled photographs of both structures underscores the relatively massive nature of urban structures– by weight and size. All information regarding the smaller "house" example is enclosed in its own box. Blue circles at the bottom compare the amount of explosives detonated in any instant and the distance between blast and structure. Resulting excitation, measured in the ground/rock at each structure at the yellow dots, is shown by the adjacent time histories; urban to the left and house to the right. Response at the red dots shows that despite urban excitation amplitudes twice those at the house, urban response was de-amplified to only 20% of the excitation, while house response was amplified to 2.4 times that of the excitation. This difference is in part the result of higher frequency (333 cycles per second, cps or Hz) urban excitation compared to the lower, 5 cps, house excitation. Urban de-amplification also results from the non-homogenous response compared to the house. Arrival times of the excitation motions at north and south end of the urban structure differ greatly as shown by the difference in arrival times of the motions at yellow, green and red dots. For the house the peaks of the yellow, green and red coincide. The difference in arrival and response times for urban structures demonstrates that the energy of the urban high frequency excitation is insufficient to produce whole body response of the massive urban structure

Urban Structures Unresponsive Compared to Houses even when excited by larger blasting vibrations because of their mass and the ultra high frequency excitation pulses

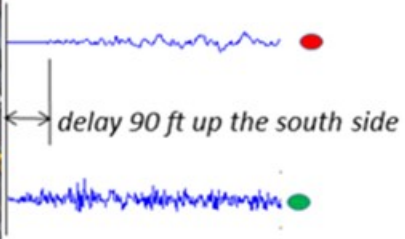

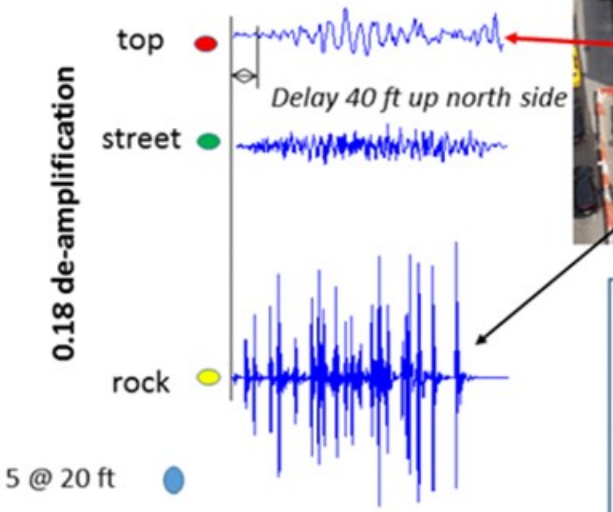

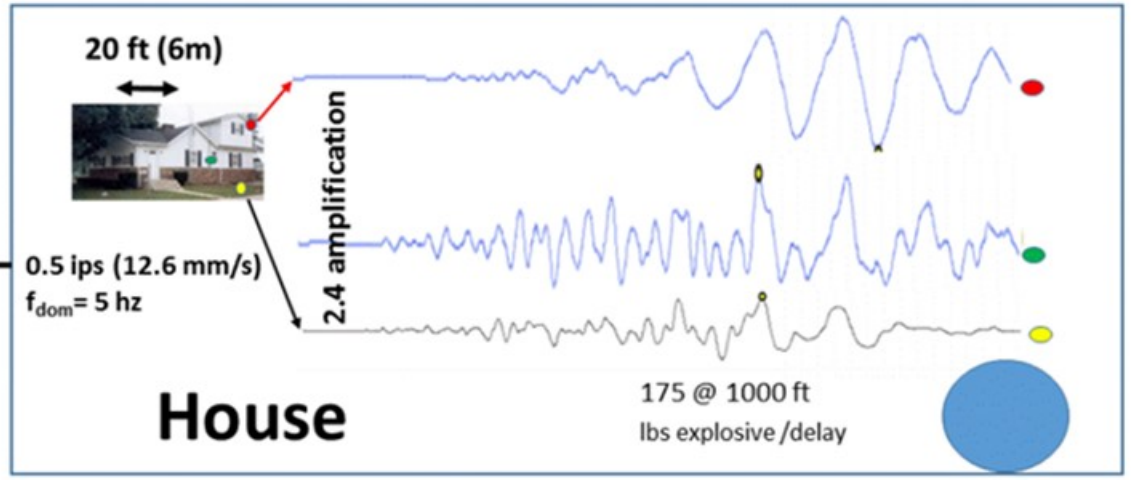

Timing, frequency and amplitudes of motions at various locations around **urban** structure show low, de-amplified response compared to the amplified response of small residential (**house**) structures even though urban excitation amplitude is 2.15 times greater than house excitation

Appendix C
Diels Data

Time Histories of the runs that provided the data to produce Table 1

Figure C1: Response to Continuous Sinusoidal Base Excitation of 0.030 cm at 1.88 Hz

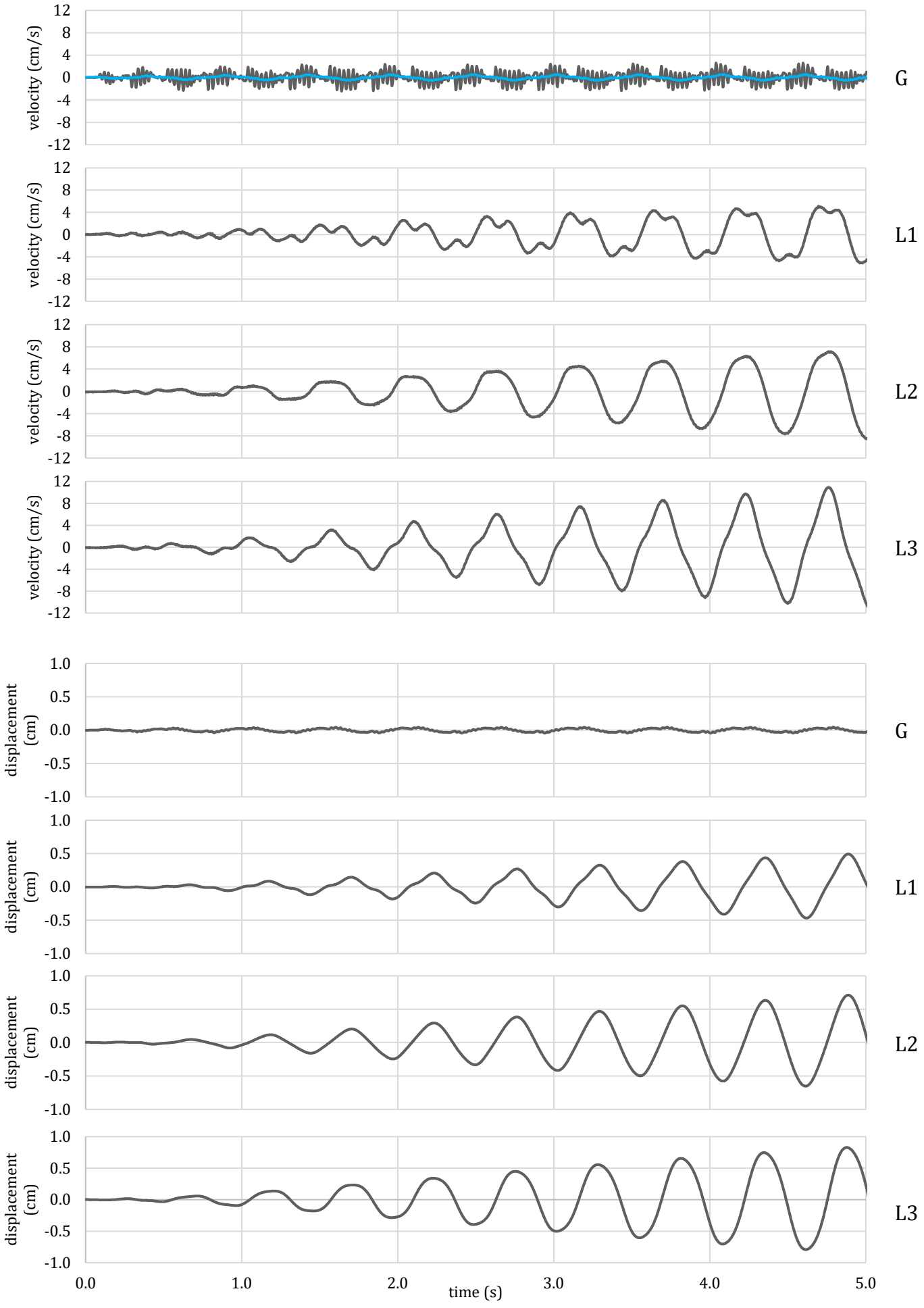

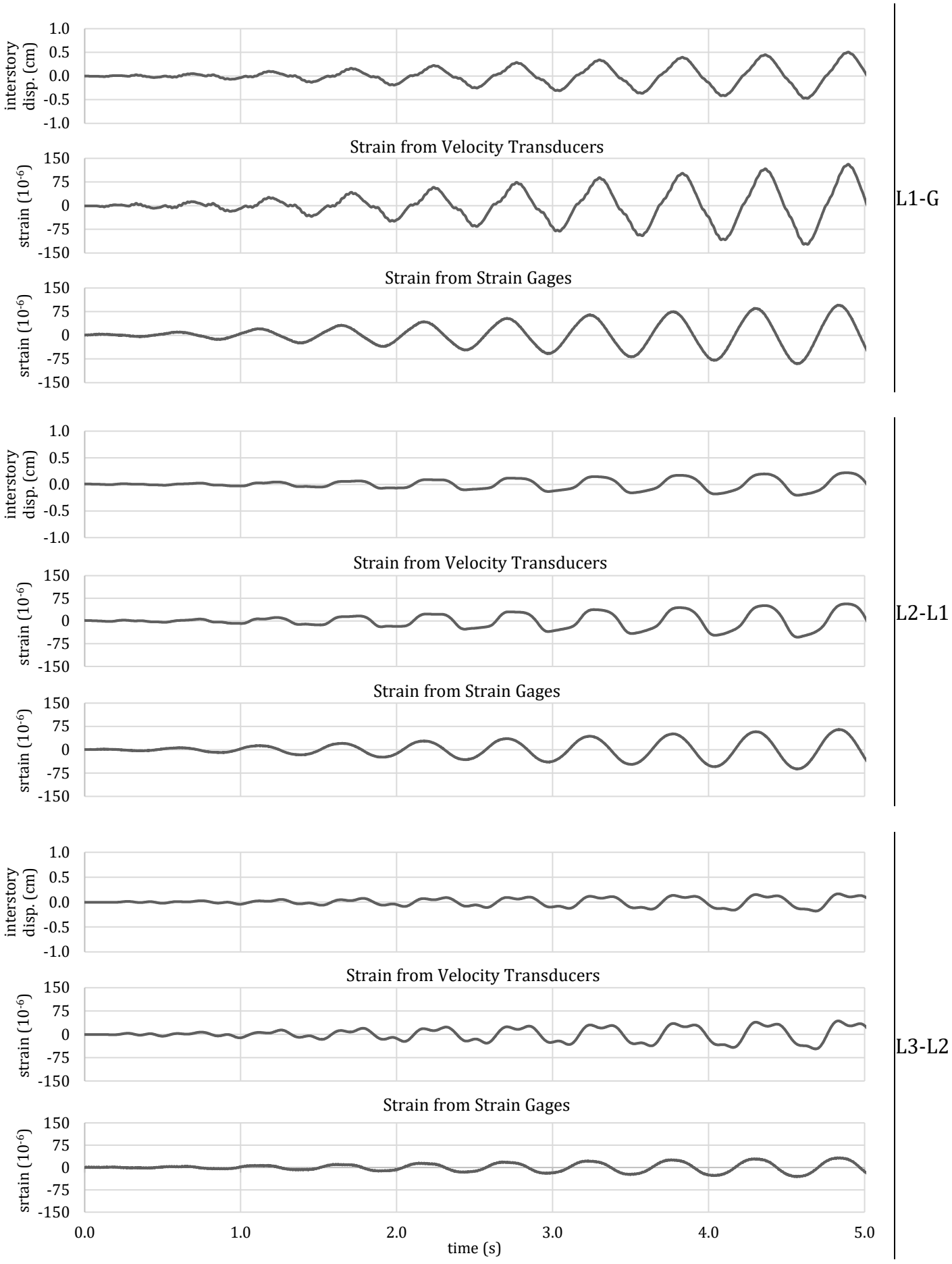
interstory disp. (cm)
1.0
0.5
0.0
-0.5
-1.0
Strain from Velocity Transducers
strain (10-6)
150
75
0
-75
-150
Strain from Strain Gages
srtain (10-6)
L1-G
L2-L1
L3-L2
0.0
1.0
2.0
3.0
4.0
5.0
time (s)

Figure C2: Response to Continuous Sinusoidal Base Excitation of 0.030 cm at 5.43 Hz

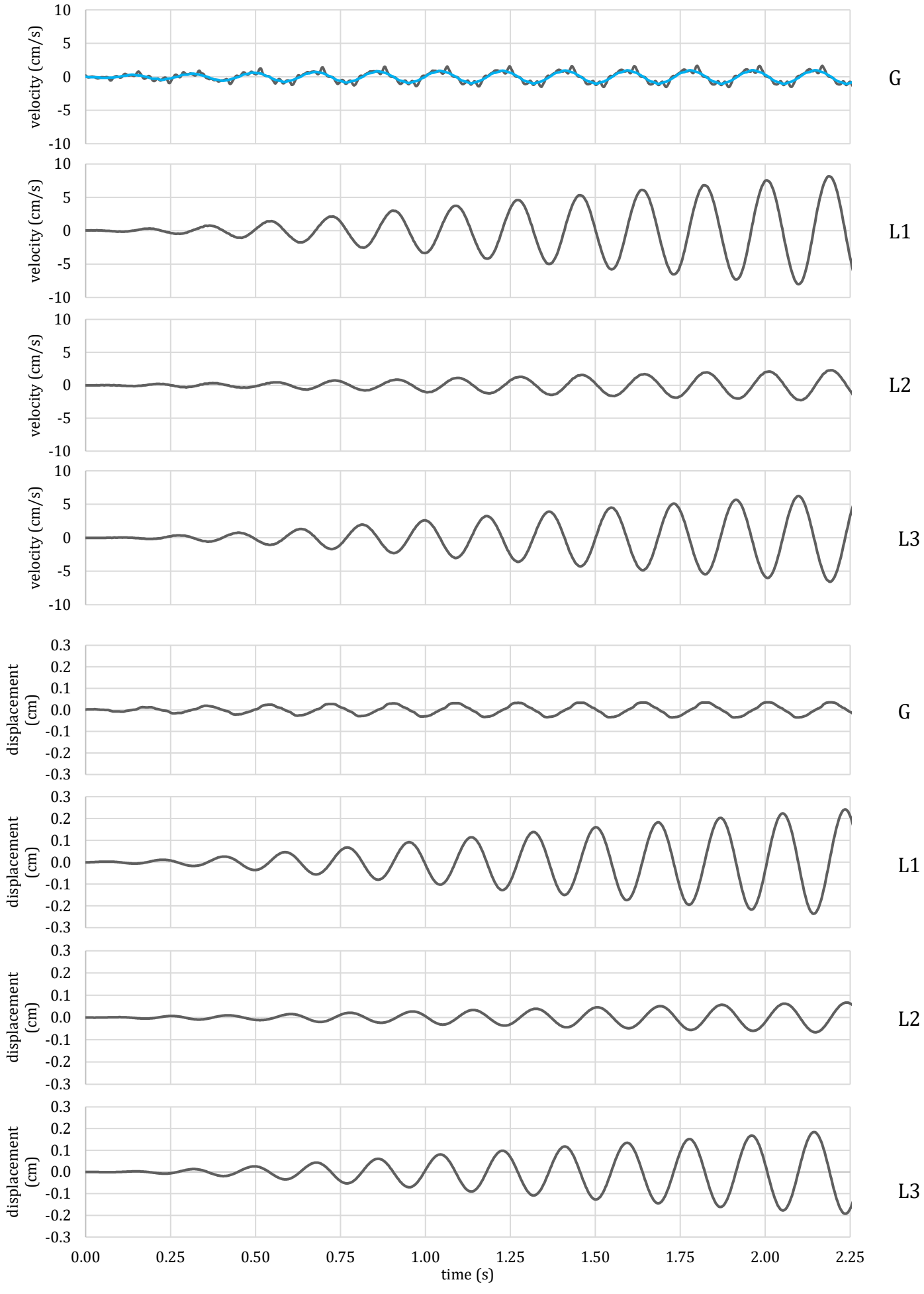

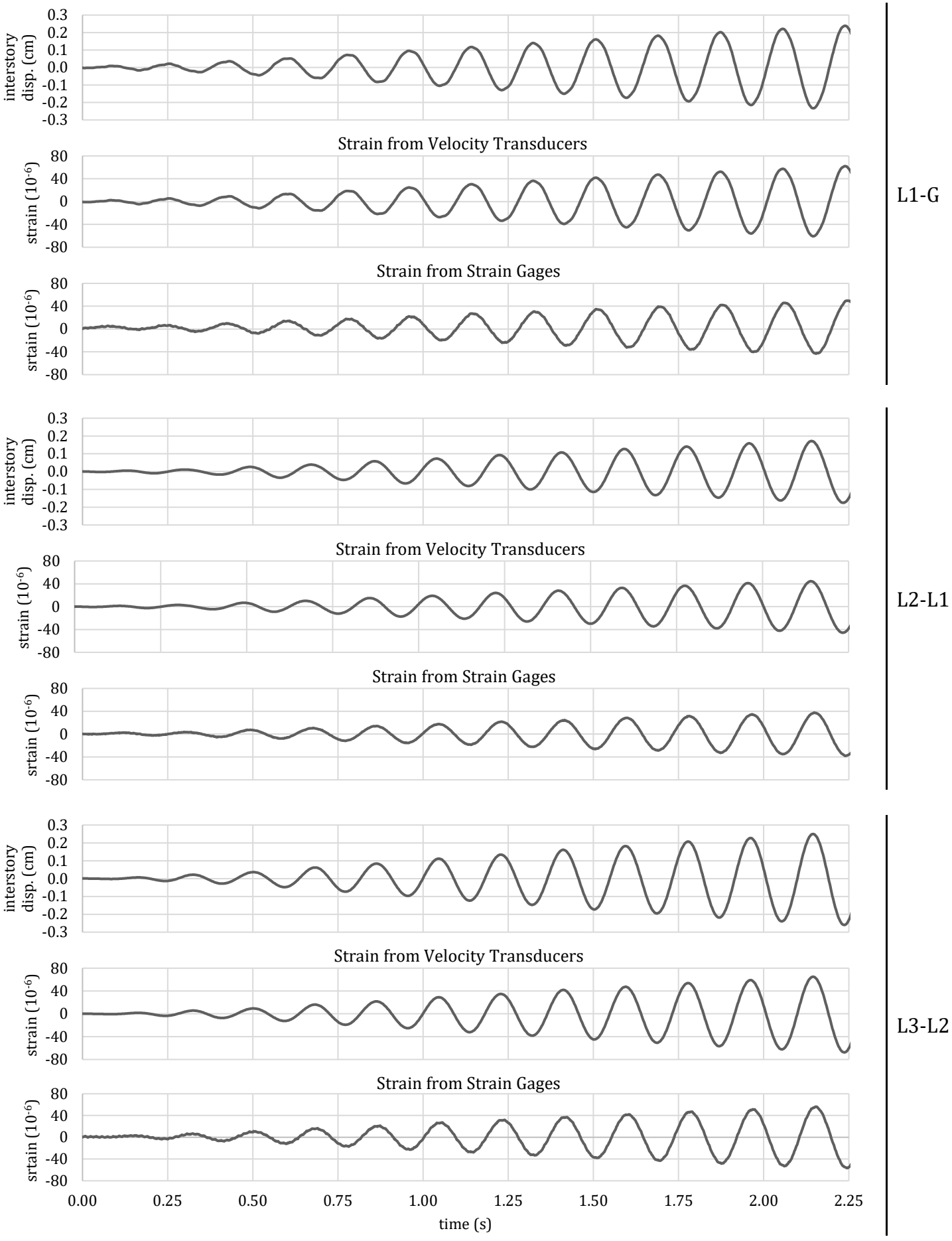
interstory disp. (cm)
0.3
0.2
0.1
0.0
-0.1
-0.2
-0.3
Strain from Velocity Transducers
strain (10-6)
80
40
0
-40
-80
Strain from Strain Gages
srtain (10-6)
80
40
0
-40
-80
L1-G
interstory disp. (cm)
0.3
0.2
0.1
0.0
-0.1
-0.2
-0.3
Strain from Velocity Transducers
strain (10-6)
80
40
0
-40
-80
Strain from Strain Gages
srtain (10-6)
80
40
0
-40
-80
L2-L1
interstory disp. (cm)
0.3
0.2
0.1
0.0
-0.1
-0.2
-0.3
Strain from Velocity Transducers
strain (10-6)
80
40
0
-40
-80
Strain from Strain Gages
srtain (10-6)
80
40
0
-40
-80
0.00
0.25
0.50
0.75
1.00
1.25
1.50
1.75
2.00
2.25
time (s)
L3-L2

Figure C3: Response to Continuous Sinusoidal Base Excitation of 0.030 cm at 8.24 Hz

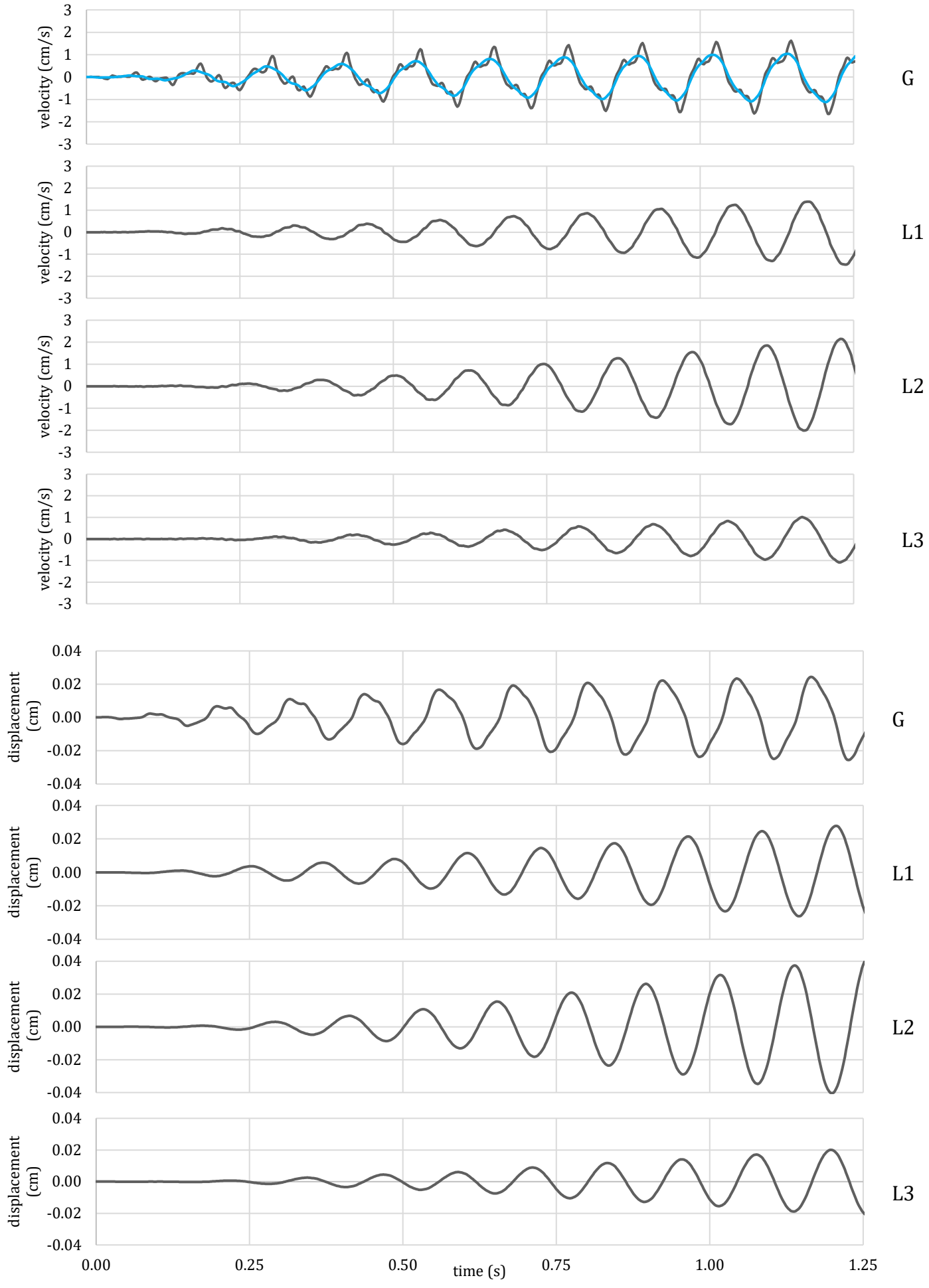

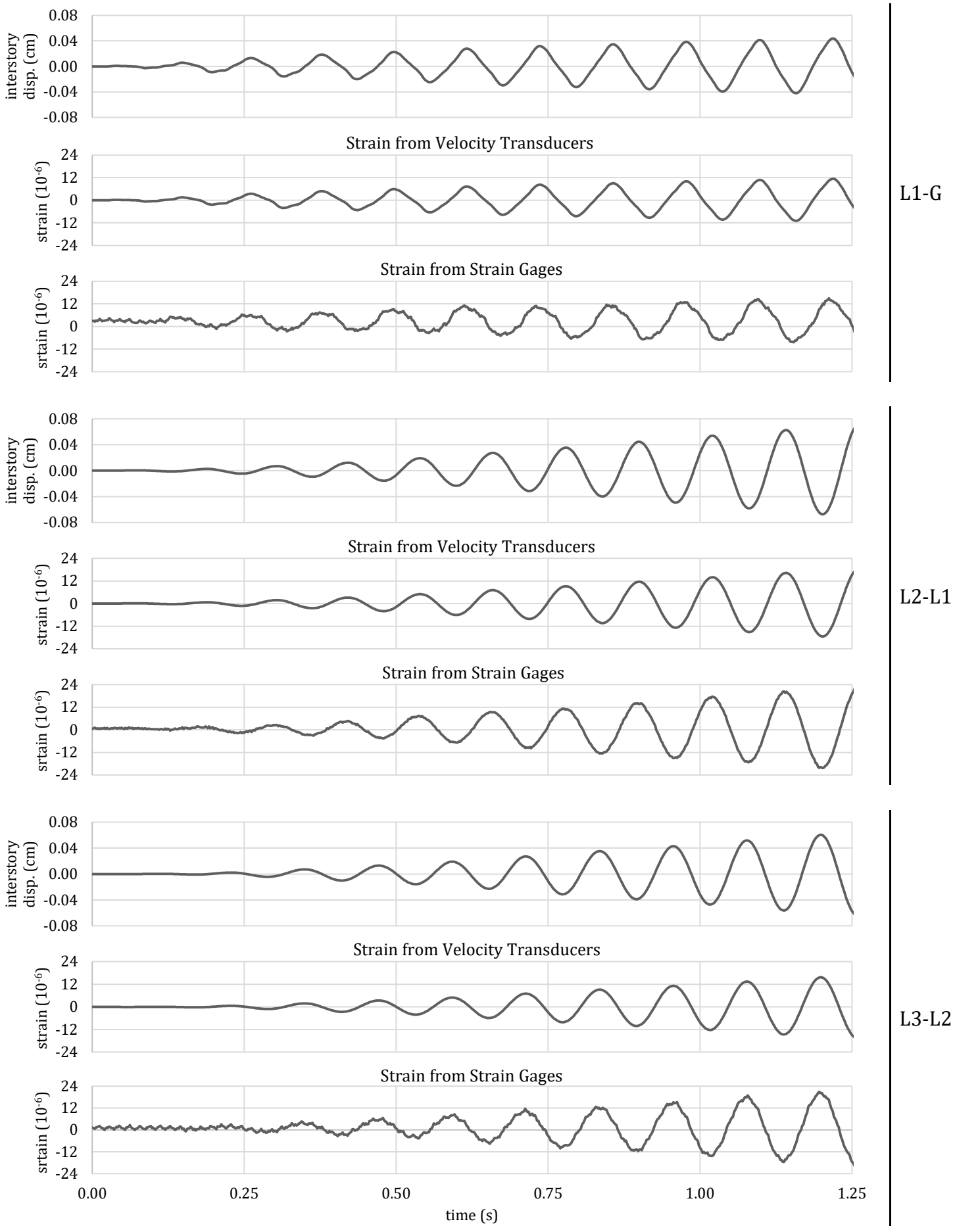
interstory disp. (cm)
0.08
0.04
0.00
-0.04
-0.08
Strain from Velocity Transducers
strain (10^{-6})
24
12
0
-12
-24
Strain from Strain Gages
srtain (10^{-6})
L1-G
L2-L1
L3-L2
0.00
0.25
0.50
0.75
1.00
1.25
time (s)

Figure C4: Response to Blast Vibration with 0.030 cm Peak Displacement (Velocity Transducers)

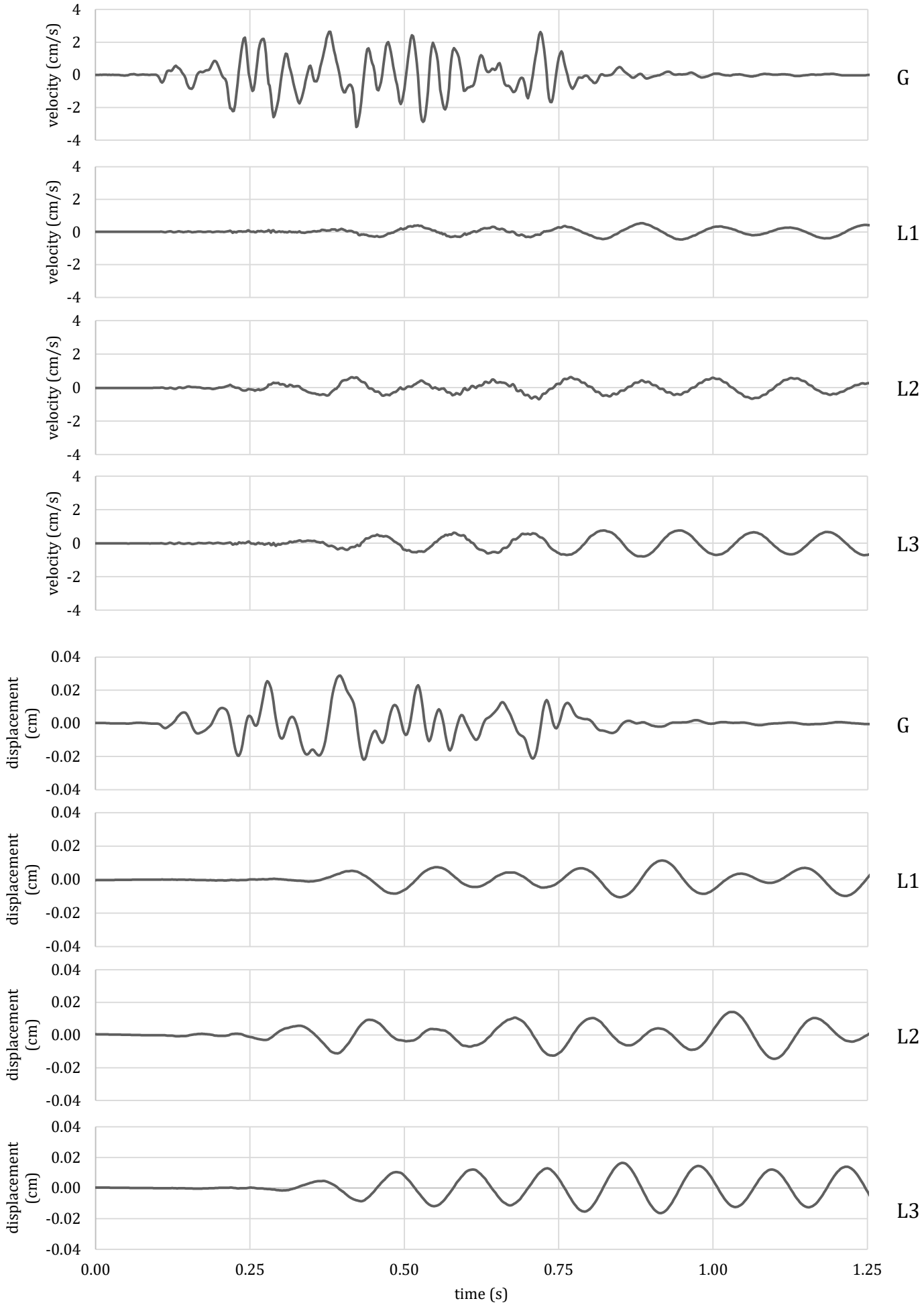

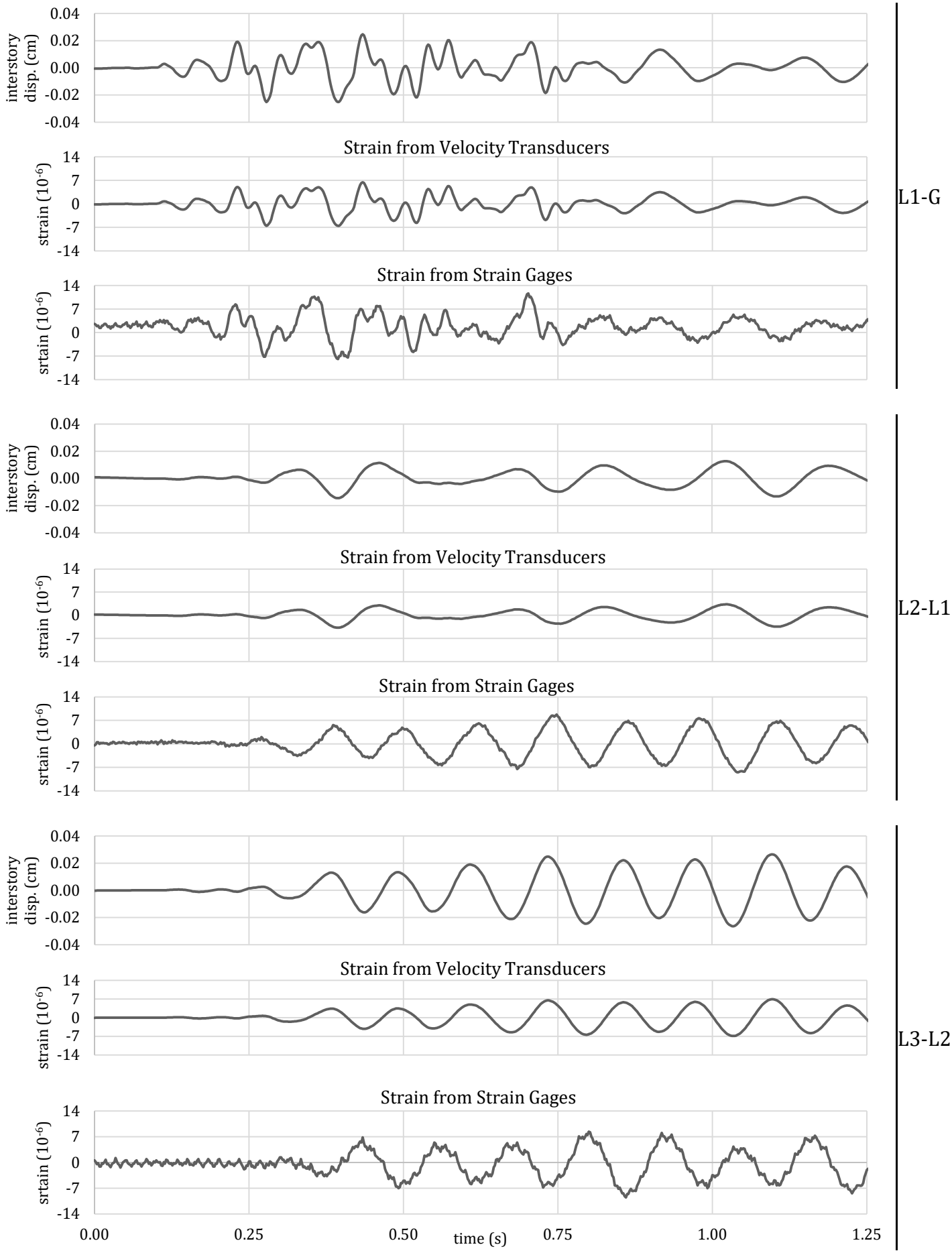
interstory disp. (cm)
0.04
0.02
0.00
-0.02
-0.04
Strain from Velocity Transducers
strain (10^{-6})
14
7
0
-7
-14
Strain from Strain Gages
srtain (10^{-6})
L1-G
L2-L1
L3-L2
0.00
0.25
0.50
0.75
1.00
1.25
time (s)

Figure C5: Response to Blast Vibration with 0.030 cm Peak Displacement (Commercial Seismograph)

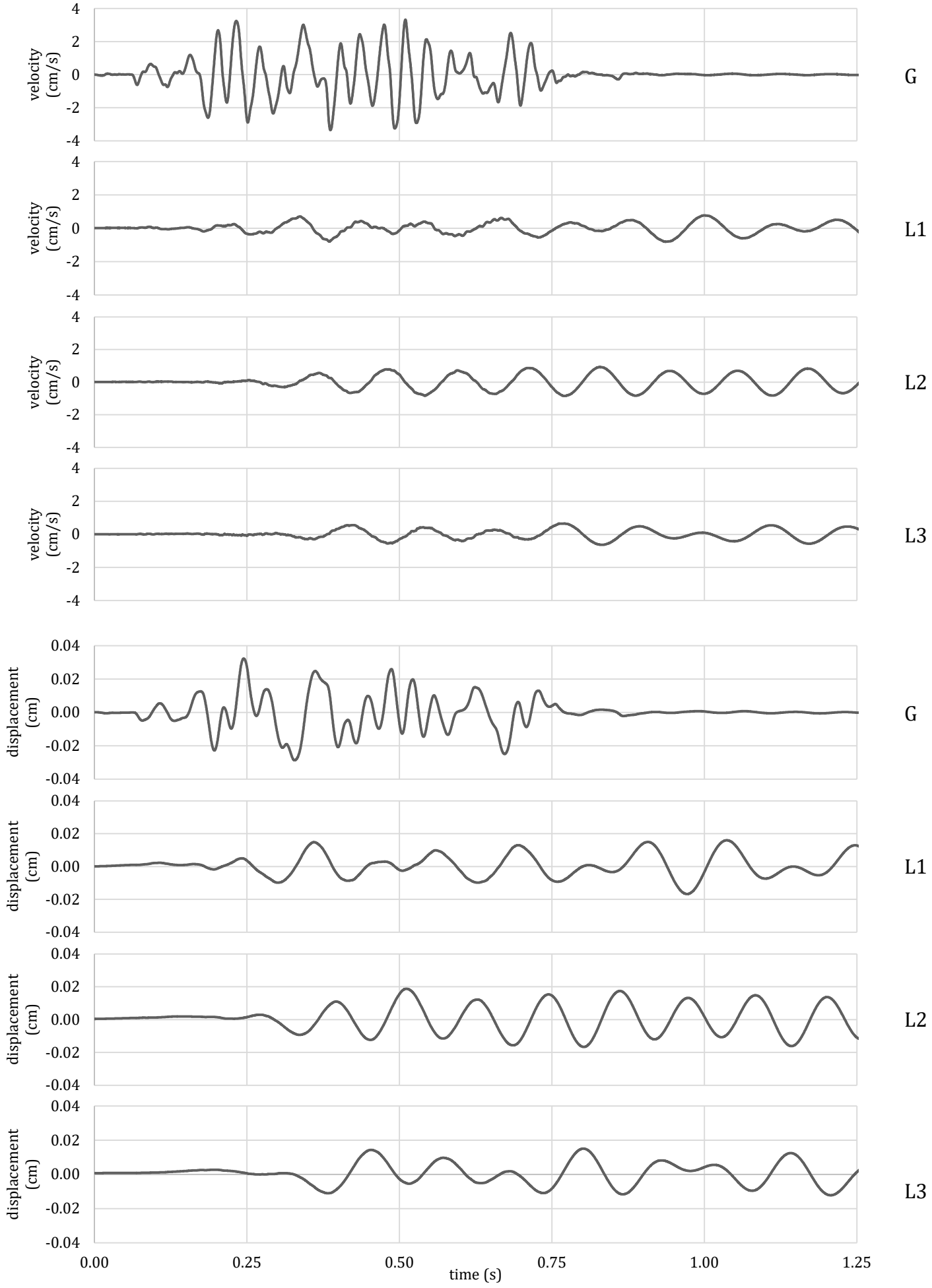

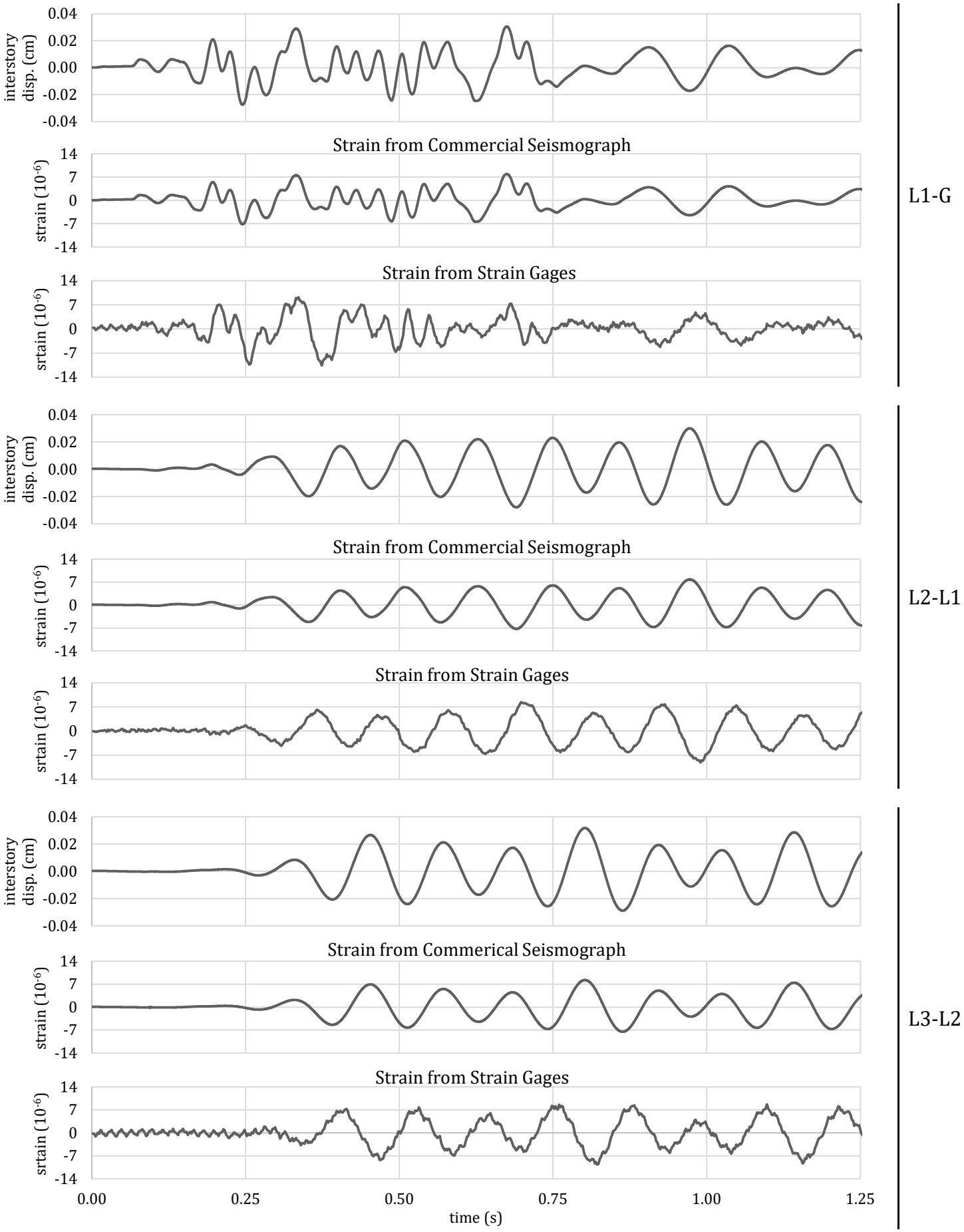
interstory disp. (cm)
0.04
0.02
0.00
-0.02
-0.04
Strain from Commercial Seismograph
strain (10-6)
14
7
0
-7
-14
Strain from Strain Gages
srtain (10-6)
L1-G
L2-L1
Strain from Commerical Seismograph
L3-L2
0.00
0.25
0.50
0.75
1.00
1.25
time (s)